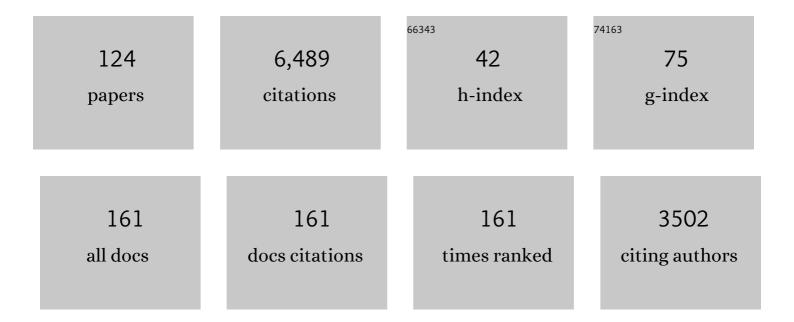
List of Publications by Year in descending order

Source: https://exaly.com/author-pdf/8990456/publications.pdf Version: 2024-02-01



M P RUPTON

#	Article	IF	CITATIONS
1	Mid-Holocene lateral collapse of Antuco volcano (Chile): debris avalanche deposit features, emplacement dynamics, and impacts. Landslides, 2022, 19, 1321-1338.	5.4	3
2	Quantification of Volcano Deformation Caused by Volatile Accumulation and Release. Geophysical Research Letters, 2022, 49, .	4.0	2
3	Dendritic crystallization in hydrous basaltic magmas controls magma mobility within the Earth's crust. Nature Communications, 2022, 13, .	12.8	17
4	Explosivity of basaltic lava fountains is controlled by magma rheology, ascent rate and outgassing. Earth and Planetary Science Letters, 2021, 553, 116658.	4.4	42
5	Synoptic analysis of a decade of daily measurements of SO <sub>2</sub> emission in the troposphere from volcanoes of the global ground-based Network for Observation of Volcanic and Atmospheric Change. Earth System Science Data, 2021, 13, 1167-1188.	9.9	31
6	Two Independent Light Dilution Corrections for the SO2 Camera Retrieve Comparable Emission Rates at Masaya Volcano, Nicaragua. Remote Sensing, 2021, 13, 935.	4.0	7
7	Volcanic Lateral Collapse Processes in Mafic Arc Edifices: A Review of Their Driving Processes, Types and Consequences. Frontiers in Earth Science, 2021, 9, .	1.8	12
8	Insights into the 9 December 2019 eruption of Whakaari/White Island from analysis of TROPOMI SO <sub>2</sub> imagery. Science Advances, 2021, 7, .	10.3	21
9	In situ quantification of crystallisation kinetics of plagioclase and clinopyroxene in basaltic magma: Implications for lava flow. Earth and Planetary Science Letters, 2021, 568, 117016.	4.4	10
10	Determining the Effect of Varying Magmatic Volatile Content on Lunar Magma Ascent Dynamics. Journal of Geophysical Research E: Planets, 2021, 126, e2021JE006939.	3.6	6
11	Pre- and syn-eruptive conditions of a basaltic Plinian eruption at Masaya Volcano, Nicaragua: The Masaya Triple Layer (2.1Âka). Journal of Volcanology and Geothermal Research, 2020, 392, 106761.	2.1	32
12	iFit: A simple method for measuring volcanic SO2 without a measured Fraunhofer reference spectrum. Journal of Volcanology and Geothermal Research, 2020, 402, 107000.	2.1	8
13	Quantifying Light Dilution in Ultraviolet Spectroscopic Measurements of Volcanic SO2 Using Dual-Band Modeling. Frontiers in Earth Science, 2020, 8, .	1.8	9
14	Conduit dynamics of highly explosive basaltic eruptions: The 1085†CE Sunset Crater sub-Plinian events. Journal of Volcanology and Geothermal Research, 2019, 387, 106658.	2.1	26
15	Mechanisms of Unrest and Eruption at Persistently Restless Volcanoes: Insights From the 2015 Eruption of Telica Volcano, Nicaragua. Geochemistry, Geophysics, Geosystems, 2019, 20, 4162-4183.	2.5	15
16	Magma fragmentation in highly explosive basaltic eruptions induced by rapid crystallization. Nature Geoscience, 2019, 12, 1023-1028.	12.9	91
17	Carbon Dioxide Emissions from Subaerial Volcanic Regions. , 2019, , 188-236.		53
18	TROPOMI enables high resolution SO2 flux observations from Mt. Etna, Italy, and beyond. Scientific Reports, 2019, 9, 957.	3.3	34

#	Article	IF	CITATIONS
19	Initial constraints on triggering mechanisms of the eruption of Fuego volcano (Guatemala) from 3 June 2018 using IASI satellite data. Journal of Volcanology and Geothermal Research, 2019, 376, 54-61.	2.1	25
20	The unexpected explosive sub-Plinian eruption of Calbuco volcano (22–23 April 2015; southern Chile): Triggering mechanism implications. Journal of Volcanology and Geothermal Research, 2019, 378, 35-50.	2.1	31
21	Unified quantitative observation of coexisting volcanic sulfur dioxide and sulfate aerosols using ground-based Fourier transform infrared spectroscopy. Atmospheric Measurement Techniques, 2019, 12, 5381-5389.	3.1	3
22	Insights into geological processes with CO2 remote sensing – A review of technology and applications. Earth-Science Reviews, 2019, 188, 389-426.	9.1	19
23	Large-area quantification of subaerial CO2 anomalies with portable laser remote sensing and 2D tomography. The Leading Edge, 2018, 37, 222a1-222a9.	0.7	1
24	Quantification of ash sedimentation dynamics through depolarisation imaging with AshCam. Scientific Reports, 2018, 8, 15680.	3.3	2
25	Coupling Between Magmatic Degassing and Volcanic Tremor in Basaltic Volcanism. Frontiers in Earth Science, 2018, 6, .	1.8	29
26	Globally Significant CO <sub>2</sub> Emissions From Katla, a Subglacial Volcano in Iceland. Geophysical Research Letters, 2018, 45, 10,332.	4.0	21
27	Crystallisation in basaltic magmas revealed via in situ 4D synchrotron X-ray microtomography. Scientific Reports, 2018, 8, 8377.	3.3	53
28	Diode laser-based gas analyser for the simultaneous measurement of CO <sub>2</sub> and HF in volcanic plumes. Atmospheric Measurement Techniques, 2018, 11, 329-339.	3.1	4
29	The effect of diffusive re-equilibration time on trace element partitioning between alkali feldspar and trachytic melts. Chemical Geology, 2018, 495, 50-66.	3.3	16
30	Tephra From the 3 March 2015 Sustained Column Related to Explosive Lava Fountain Activity at Volcán Villarrica (Chile). Frontiers in Earth Science, 2018, 6, .	1.8	20
31	Ground-Based Measurements of the 2014–2015 Holuhraun Volcanic Cloud (Iceland). Geosciences (Switzerland), 2018, 8, 29.	2.2	35
32	Ground-Based Remote Sensing of Volcanic CO2 Fluxes at Solfatara (Italy)—Direct Versus Inverse Bayesian Retrieval. Remote Sensing, 2018, 10, 125.	4.0	1
33	SO2 emissions, plume heights and magmatic processes inferred from satellite data: The 2015 Calbuco eruptions. Journal of Volcanology and Geothermal Research, 2018, 361, 12-24.	2.1	24
34	CO <sub>2</sub> flux from Javanese mud volcanism. Journal of Geophysical Research: Solid Earth, 2017, 122, 4191-4207.	3.4	9
35	Retrieval and intercomparison of volcanic SO2 injection height and eruption time from satellite maps and ground-based observations. Journal of Volcanology and Geothermal Research, 2017, 331, 79-91.	2.1	22
36	Numerical investigation of permeability models for low viscosity magmas: Application to the 2007 Stromboli effusive eruption. Earth and Planetary Science Letters, 2017, 473, 279-290.	4.4	17

#	Article	IF	CITATIONS
37	Portable laser spectrometer for airborne and ground-based remote sensing of geological CO_2 emissions. Optics Letters, 2017, 42, 2782.	3.3	9
38	From magma ascent to ash generation: investigating volcanic conduit processes by integrating experiments, numerical modeling, and observations. Annals of Geophysics, 2017, 60, .	1.0	5
39	Increasing CO <sub>2</sub> flux at Pisciarelli, Campi Flegrei, Italy. Solid Earth, 2017, 8, 1017-1024.	2.8	11
40	2-D tomography of volcanic CO <sub>2</sub> from scanning hard-target differential absorption lidar: the case of Solfatara, Campi Flegrei (Italy). Atmospheric Measurement Techniques, 2016, 9, 5721-5734.	3.1	5
41	Quantitative Ground-Based Imaging ofÂVolcanic Ash. , 2016, , 175-185.		0
42	Role of syn-eruptive plagioclase disequilibrium crystallization in basaltic magma ascent dynamics. Nature Communications, 2016, 7, 13402.	12.8	61
43	A new frontier in CO2 flux measurements using a highly portable DIAL laser system. Scientific Reports, 2016, 6, 33834.	3.3	30
44	Degassing dynamics of basaltic lava lake at a top-ranking volatile emitter: Ambrym volcano, Vanuatu arc. Earth and Planetary Science Letters, 2016, 448, 69-80.	4.4	41
45	Gradual caldera collapse at BÃ <sub>i</sub> rdarbunga volcano, Iceland, regulated by lateral magma outflow. Science, 2016, 353, aaf8988.	12.6	230
46	Eruption dynamics of the 22–23 April 2015 Calbuco Volcano (Southern Chile): Analyses of tephra fall deposits. Journal of Volcanology and Geothermal Research, 2016, 317, 15-29.	2.1	94
47	Magma Degassing at Piton de la Fournaise Volcano. Active Volcanoes of the World, 2016, , 203-222.	1.4	23
48	Toward continuous quantification of lava extrusion rate: Results from the multidisciplinary analysis of the 2 January 2010 eruption of Piton de la Fournaise volcano, La Réunion. Journal of Geophysical Research: Solid Earth, 2015, 120, 3026-3047.	3.4	23
49	MeMoVolc consensual document: a review of cross-disciplinary approaches to characterizing small explosive magmatic eruptions. Bulletin of Volcanology, 2015, 77, 1.	3.0	22
50	Quantification of gas and solid emissions during Strombolian explosions using simultaneous sulphur dioxide and infrared camera observations. Journal of Volcanology and Geothermal Research, 2015, 300, 167-174.	2.1	16
51	Quantitative imaging of volcanic plumes — Results, needs, and future trends. Journal of Volcanology and Geothermal Research, 2015, 300, 7-21.	2.1	26
52	Open-path FTIR spectroscopy of magma degassing processes during eight lava fountains on Mount Etna. Earth and Planetary Science Letters, 2015, 413, 123-134.	4.4	37
53	Volcanological applications of SO 2 cameras. Journal of Volcanology and Geothermal Research, 2015, 300, 2-6.	2.1	21
54	Validation of the SO 2 camera for high temporal and spatial resolution monitoring of SO 2 emissions. Journal of Volcanology and Geothermal Research, 2015, 300, 37-47.	2.1	18

#	Article	IF	CITATIONS
55	SO 2 emissions at Semeru volcano, Indonesia: Characterization and quantification of persistent and periodic explosive activity. Journal of Volcanology and Geothermal Research, 2015, 300, 121-128.	2.1	21
56	SO 2 flux monitoring at Stromboli with the new permanent INGV SO 2 camera system: A comparison with the FLAME network and seismological data. Journal of Volcanology and Geothermal Research, 2015, 300, 95-102.	2.1	24
57	Temperature evolution during magma ascent in basaltic effusive eruptions: A numerical application to Stromboli volcano. Earth and Planetary Science Letters, 2015, 426, 89-100.	4.4	61
58	Differential absorption lidar for volcanic CO_2 sensing tested in an unstable atmosphere. Optics Express, 2015, 23, 6634.	3.4	32
59	Emission of gas and atmospheric dispersion of SO <sub>2</sub> during the December 2013 eruption at San Miguel volcano (El Salvador, Central America). Geophysical Research Letters, 2015, 42, 5847-5854.	4.0	16
60	Intercomparison of SO 2 camera systems for imaging volcanic gas plumes. Journal of Volcanology and Geothermal Research, 2015, 300, 22-36.	2.1	42
61	Conduit convection driving persistent degassing at basaltic volcanoes. Journal of Volcanology and Geothermal Research, 2014, 283, 19-35.	2.1	38
62	Composition and flux of explosive gas release at LUSI mud volcano ( <scp>E</scp> ast <scp>J</scp> ava,) Tj ETQq	0	/Qyerlock 10
63	Gas Flux Rate and Migration of the Magma Column. Geophysical Monograph Series, 2013, , 259-267.	0.1	2
64	Evidence for a recent change in the shallow plumbing system of Mt. Etna (Italy): Gas geochemistry and structural data during 2001–2005. Journal of Volcanology and Geothermal Research, 2013, 251, 90-97.	2.1	12
65	Deep Carbon Emissions from Volcanoes. Reviews in Mineralogy and Geochemistry, 2013, 75, 323-354.	4.8	313
66	New insights into volcanic processes at Stromboli from Cerberus, a remote-controlled open-path FTIR scanner system. Journal of Volcanology and Geothermal Research, 2013, 249, 66-76.	2.1	34
67	Investigating the effect of aerosol droplets in a volcanic plume for increasing sensitivity of a CO <sub>2</sub> DIAL measurement. Proceedings of SPIE, 2013, , .	0.8	1
68	The coupling between very long period seismic events, volcanic tremor, and degassing rates at Mount Etna volcano. Journal of Geophysical Research: Solid Earth, 2013, 118, 4910-4921.	3.4	38
69	11. Deep Carbon Emissions from Volcanoes. , 2013, , 323-354.		12

70	Field determination of biomass burning emission ratios and factors via open-path FTIR spectroscopy and fire radiative power assessment: headfire, backfire and residual smouldering combustion in African savannahs. Atmospheric Chemistry and Physics, 2011, 11, 11591-11615.	4.9	64
71	Coupled use of COSPEC and satellite measurements to define the volumetric balance during effusive eruptions at Mt. Etna, Italy. Journal of Volcanology and Geothermal Research, 2011, 205, 47-53.	2.1	25
72	Reconstruction of SO2 flux emission chronology from space-based measurements. Journal of Volcanology and Geothermal Research, 2011, 206, 80-87.	2.1	43

#	Article	IF	CITATIONS
73	First observational evidence for the CO <sub>2</sub> -driven origin of Stromboli's major explosions. Solid Earth, 2011, 2, 135-142.	2.8	56
74	Measuring volcanic degassing of SO2 in the lower troposphere with ASTER band ratios. Journal of Volcanology and Geothermal Research, 2010, 194, 42-54.	2.1	47
75	Unravelling the processes controlling gas emissions from the central and northeast craters of Mt. Etna. Journal of Volcanology and Geothermal Research, 2010, 198, 368-376.	2.1	50
76	Unusually large magmatic CO <sub>2</sub> gas emissions prior to a basaltic paroxysm. Geophysical Research Letters, 2010, 37, .	4.0	95
77	SO2 flux from Stromboli during the 2007 eruption: Results from the FLAME network and traverse measurements. Journal of Volcanology and Geothermal Research, 2009, 182, 214-220.	2.1	109
78	The role of syn-eruptive vesiculation on explosive basaltic activity at Mt. Etna, Italy. Journal of Volcanology and Geothermal Research, 2009, 179, 265-269.	2.1	31
79	Novel retrieval of volcanic SO2 abundance from ultraviolet spectra. Journal of Volcanology and Geothermal Research, 2009, 181, 141-153.	2.1	58
80	Three-years of SO2 flux measurements of Mt. Etna using an automated UV scanner array: Comparison with conventional traverses and uncertainties in flux retrieval. Journal of Volcanology and Geothermal Research, 2009, 183, 76-83.	2.1	120
81	Quantification of the gas mass emitted during single explosions on Stromboli with the SO2 imaging camera. Journal of Volcanology and Geothermal Research, 2009, 188, 395-400.	2.1	84
82	Visualising volcanic gas plumes with virtual globes. Computers and Geosciences, 2009, 35, 1837-1842.	4.2	15
83	The 16 November 2006 flank collapse of the southâ€east crater at Mount Etna, Italy: Study of the deposit and hazard assessment. Journal of Geophysical Research, 2009, 114, .	3.3	30
84	Investigation into magma degassing at Nyiragongo volcano, Democratic Republic of the Congo. Geochemistry, Geophysics, Geosystems, 2008, 9, .	2.5	102
85	Scanning tomography of SO <sub>2</sub> distribution in a volcanic gas plume. Geophysical Research Letters, 2008, 35, .	4.0	22
86	Total volatile flux from Mount Etna. Geophysical Research Letters, 2008, 35, .	4.0	112
87	Magmatic Gas Composition Reveals the Source Depth of Slug-Driven Strombolian Explosive Activity. Science, 2007, 317, 227-230.	12.6	315
88	The role of gas percolation in quiescent degassing of persistently active basaltic volcanoes. Earth and Planetary Science Letters, 2007, 264, 46-60.	4.4	147
89	The SO2camera: A simple, fast and cheap method for ground-based imaging of SO2in volcanic plumes. Geophysical Research Letters, 2006, 33, .	4.0	166
90	Effects of a volcanic plume on thermal imaging data. Geophysical Research Letters, 2006, 33, .	4.0	53

#	Article	IF	CITATIONS
91	Continuous soil radon monitoring during the July 2006 Etna eruption. Geophysical Research Letters, 2006, 33, .	4.0	82
92	Rapid FTIR sensing of volcanic gases released by Strombolian explosions at Yasur volcano, Vanuatu. Applied Physics B: Lasers and Optics, 2006, 85, 453-460.	2.2	84
93	Effusive to explosive transition during the 2003 eruption of Stromboli volcano. Geology, 2005, 33, 341.	4.4	119
94	Spectroscopic evidence for a lava fountain driven by previously accumulated magmatic gas. Nature, 2005, 433, 407-410.	27.8	243
95	A multi-disciplinary study of the 2002?03 Etna eruption: insights into a complex plumbing system. Bulletin of Volcanology, 2005, 67, 314-330.	3.0	271
96	Chronology and complex volcanic processes during the 2002-2003 flank eruption at Stromboli volcano (Italy) reconstructed from direct observations and surveys with a handheld thermal camera. Journal of Geophysical Research, 2005, 110, .	3.3	151
97	Etna 2004–2005: An archetype for geodynamically-controlled effusive eruptions. Geophysical Research Letters, 2005, 32, .	4.0	120
98	Correction to "Chronology and complex volcanic processes during the 2002-2003 flank eruption at Stromboli volcano (Italy) reconstructed from direct observations and surveys with a handheld thermal camera― Journal of Geophysical Research, 2005, 110, .	3.3	7
99	Intercomparison of volcanic gas monitoring methodologies performed on Vulcano Island, Italy. Geophysical Research Letters, 2004, 31, .	4.0	29
100	High spatial resolution radon measurements reveal hidden active faults on Mt. Etna. Geophysical Research Letters, 2004, 31, n/a-n/a.	4.0	78
101	Volcanic gas emissions from the summit craters and flanks of Mt. Etna, 1987–2000. Geophysical Monograph Series, 2004, , 111-128.	0.1	64
102	2001 flank eruption of the alkali- and volatile-rich primitive basalt responsible for Mount Etna's evolution in the last three decades. Earth and Planetary Science Letters, 2004, 228, 1-17.	4.4	216
103	Changes in gas composition prior to a minor explosive eruption at Masaya volcano, Nicaragua. Journal of Volcanology and Geothermal Research, 2003, 126, 327-339.	2.1	91
104	Sulphur dioxide fluxes from Mount Etna, Vulcano, and Stromboli measured with an automated scanning ultraviolet spectrometer. Journal of Geophysical Research, 2003, 108, .	3.3	61
105	FTIR remote sensing of fractional magma degassing at Mount Etna, Sicily. Geological Society Special Publication, 2003, 213, 281-293.	1.3	51
106	Compositional variation in tropospheric volcanic gas plumes: evidence from ground-based remote sensing. Geological Society Special Publication, 2003, 213, 349-369.	1.3	20
107	Variation in HCl/SO2 gas ratios observed by Fourier transform spectroscopy at Soufrière Hills Volcano, Montserrat. Geological Society Memoir, 2002, 21, 621-639.	1.7	20
108	Field measurements of volcanic gases using tunable diode laser based mid-infrared and Fourier transform infrared spectrometers. Optics and Lasers in Engineering, 2002, 37, 171-186.	3.8	56

#	Article	IF	CITATIONS
109	Open-path Fourier transform spectroscopy of gas emissions from Oldoinyo Lengai volcano, Tanzania. Optics and Lasers in Engineering, 2002, 37, 203-214.	3.8	27
110	Diurnal changes in volcanic plume chemistry observed by lunar and solar occultation spectroscopy. Geophysical Research Letters, 2001, 28, 843-846.	4.0	39
111	Open-path Fourier transform infrared spectroscopy of SO2: An empirical error budget analysis, with implications for volcano monitoring. Journal of Geophysical Research, 2001, 106, 27647-27659.	3.3	37
112	Volcanic gas emission rates measured by solar occultation spectroscopy. Geophysical Research Letters, 2001, 28, 3131-3134.	4.0	40
113	The relationship between degassing and ground deformation at Soufriere Hills Volcano, Montserrat. Journal of Volcanology and Geothermal Research, 2000, 98, 117-126.	2.1	80
114	Remote sensing of CO2 and H2O emission rates from Masaya volcano, Nicaragua. Geology, 2000, 28, 915.	4.4	146
115	Remote sensing of CO2 and H2O emission rates from Masaya volcano, Nicaragua. Geology, 2000, 28, 915-918.	4.4	19
116	Origin, effects of Masaya Volcano's continued unrest probed in Nicaragua. Eos, 1999, 80, 575-581.	0.1	36
117	Stable gas plume composition measured by OP-FTIR spectroscopy at Masaya Volcano, Nicaragua, 1998-1999. Geophysical Research Letters, 1999, 26, 3497-3500.	4.0	59
118	Remote measurements of volcanic gas compositions by solar occultation spectroscopy. Nature, 1998, 396, 567-570.	27.8	171
119	Remote measurement of volcanic gases by Fourier transform infrared spectroscopy. Applied Physics B: Lasers and Optics, 1998, 67, 505-515.	2.2	133
120	The effect of uncertainties in kinetic and photochemical data on model predictions of stratospheric ozone depletion. Journal of Geophysical Research, 1997, 102, 25537-25542.	3.3	18
121	On the use of HF as a reference for the comparison of stratospheric observations and models. Journal of Geophysical Research, 1997, 102, 12901-12919.	3.3	35
122	Crater Gas Emissions and the Magma Feeding System of Stromboli Volcano. Geophysical Monograph Series, 0, , 65-80.	0.1	16
123	Volcanic and Seismic Activity at Stromboli Preceding the 2002-2003 Flank Eruption. Geophysical Monograph Series, 0, , 93-104.	0.1	7
124	Behaviors of Redox-Sensitive Components in the Volcanic Plume at Masaya Volcano, Nicaragua: H2 Oxidation and CO Preservation in Air. Frontiers in Earth Science, 0, 10, .	1.8	1